

Miniband transport and oscillations in semiconductor superlattices

Álvaro Perales¹, Luis L Bonilla² and Ramón Escobedo²

¹ Departamento de Automática, Escuela Politécnica, Universidad de Alcalá,
28871 Alcalá de Henares, Spain

² Departamento de Matemáticas, Escuela Politécnica Superior, Universidad Carlos III de
Madrid, Avenida de la Universidad 30, 28911 Leganés, Spain

E-mail: alvaro.perales@uah.es

Received 1 October 2003

Published 20 February 2004

Online at stacks.iop.org/Nano/15/S229 (DOI: 10.1088/0957-4484/15/4/021)

Abstract

We present and analyse solutions of a recent derivation of a drift-diffusion model of miniband transport in strongly coupled superlattices. The model is obtained from a single-miniband Boltzmann–Poisson transport equation with a BGK (Bhatnagar–Gross–Krook) collision term by means of a consistent Chapman–Enskog expansion. The reduced drift-diffusion equation is solved numerically and travelling field domains and current oscillations are obtained. A broad range of frequencies can be achieved, depending on the model parameters, in good agreement with available experiments on GaAs/AlAs superlattices.

1. Introduction

Since Esaki and Tsu's proposal [1], charge transport in semiconductor superlattices (SLs) has attracted great interest, as shown by the numerous experimental results, theoretical analyses and simulations of rate equation models [2–4]. As often happens, these models have not been derived from more fundamental 'first-principles formulations' such as kinetic theory. In strongly coupled SLs, barriers are so thin that the wavefunctions of electrons located in different wells strongly overlap. At low applied electric fields, this produces wide minibands extending over the whole SL and electron transport is well described by semiclassical kinetic equations for miniband distribution functions. Practical models to analyse nonlinear transport are typically simpler, either of drift-diffusion type [5] or hydrodynamic models [6, 7]. The latter are considerably more complicated and have been solved numerically, but few analytical results have been obtained.

Models based on drift-diffusion equations (DDEs) typically use a drift velocity obtained from a simplified kinetic equation and a diffusion coefficient that obeys the Einstein relation [8]. The resulting model is a variant of the well-known Kroemer DDE for the Gunn effect in bulk n-GaAs [9]. For the large fields involved and for the non-parabolic SL miniband energy, using an Einstein relation to figure out the diffusion coefficient is questionable [10] and even incorrect except in a particular limit of high temperatures. A consistent derivation

of a DDE for strongly coupled SLs from a kinetic equation is missing.

Recently, we have provided such a derivation in a high-field hyperbolic limit [11]. We have solved numerically the resulting DDE together with boundary and initial conditions. The solutions consist of self-sustained oscillations of the current through the SL, mediated by periodic motion of pulses of the electric field inside the SL. These solutions quantitatively agree with experimental results.

2. Model: from Boltzmann–Poisson to drift-diffusion

The derivation starts from a semiclassical Boltzmann–Poisson system that describes one-dimensional electron transport in the lowest miniband of a strongly coupled superlattice. The equations are as follows:

$$\frac{\partial f}{\partial t} + v(k) \frac{\partial f}{\partial x} + \frac{eF}{\hbar} \frac{\partial f}{\partial k} = -v_e(f - f^{\text{FD}}) - v_l \frac{f(x, k, t) - f(x, -k, t)}{2}, \quad (1)$$

$$\varepsilon \frac{\partial F}{\partial x} = \frac{e}{l} (n - N_D), \quad (2)$$

$$n(x, t) = \frac{l}{2\pi} \int_{-\pi/l}^{\pi/l} f(x, k, t) dk$$

Table 1. Variables and parameters for equations (1)–(6).

F	Electric field	l	SL period
\hbar	Planck constant	ε	Dielectric constant
e	Negative electric charge	N_D	2D doping density
m^*	GaAs effective mass	k_B	Boltzmann constant
μ	Chemical potential	T	Temperature
Δ	Miniband width	$\mathcal{E}(k)$	Dispersion relation
$\nu_{e,i}$	Scattering rates	$v(k)$	Group velocity

$$= \frac{l}{2\pi} \int_{-\pi/l}^{\pi/l} f^{\text{FD}}(k; n) dk, \quad (3)$$

$$f^{\text{FD}}(k; n) = \frac{m^* k_B T}{\pi \hbar^2} \ln \left[1 + \exp \left(\frac{\mu - \mathcal{E}(k)}{k_B T} \right) \right], \quad (4)$$

$$\mathcal{E}(k) = \frac{\Delta}{2} (1 - \cos kl), \quad (5)$$

$$v(k) = \frac{1}{\hbar} \frac{\partial \mathcal{E}(k)}{\partial k} = \frac{\Delta l}{2\hbar} \sin kl. \quad (6)$$

Here $f(x, k, t)$, $f^{\text{FD}}(k; n)$ and $n(x, t)$ are the electronic distribution function, Fermi–Dirac distribution function (equilibrium) and 2D electronic density, respectively. The other variables, parameters and constants are listed in table 1.

Equation (1) is the semiclassical Boltzmann equation for miniband transport with two collision terms. The first collision term has a BGK (Bhatnagar–Gross–Krook) form [12] and it represents energy relaxation towards a 1D effective Fermi–Dirac distribution $f^{\text{FD}}(k; n)$ (local equilibrium), with collision frequency ν_e . The second term accounts for impurity elastic collisions with frequency ν_i . Equation (2) is the Poisson equation and equation (3) relates electron density with exact and FD distribution functions, thereby preserving charge continuity as in the BGK model [12]. Equation (4) is the 1D Fermi–Dirac model, (5) is the tight-binding dispersion relation and (6) is the group velocity.

The Boltzmann–Poisson system (1)–(6) cannot be solved analytically and numerical solutions are costly. To derive a reduced balance equation for n we shall assume that the electric field contribution in equation (1) is comparable to the collision terms and that these terms dominate the other two. This is the so-called *hyperbolic limit* in which the ratio of $\partial f / \partial t$ or $v(k) \partial f / \partial x$ to $(eF/\hbar) \partial f / \partial k$ is of the order of $\epsilon \ll 1$. Let v_M and F_M be typical scales of electron velocity and electric field, respectively, e.g. the positive values at which the (zeroth-order) drift velocity reaches its maximum. From these scales, we obtain the characteristic space and timescales by assuming that t_0 is the time it takes an electron with speed v_M to traverse a distance $x_0 = \varepsilon F_M l / (e N_D)$, over which the field variation is of the order of F_M . The expressions for v_M and F_M in terms of fundamental parameters will be derived below. In the hyperbolic limit, the mean free time between collisions, $\nu_e^{-1} \sim \hbar / (e F_M l) = t_1$, is much shorter than the dielectric time $t_0 = \varepsilon F_M l / (e N_D v_M)$ and $\epsilon = t_1 / t_0 = \hbar v_M N_D / (\varepsilon F_M^2 l^2) \ll 1$ (see [14]³). All units are listed in table 2, in which the numerical values correspond to one of the SLs of [13].

³ This criterion yields $\epsilon = 0.38$ for the sample in table 3 with $\Delta = 97.99$ meV, overestimating the ratio of the drift term $v(k) \partial f / \partial x$ to the term $(eF/\hbar) \partial f / \partial k$, or to the collision terms. The asymptotic description of the Gunn effect in [14] shows that, during self-sustained or driven current oscillations, the field variation is larger than F_M and the average drift velocity is smaller than v_M . A more realistic estimation yields a 20 times smaller ϵ .

Table 2. Characteristic scales and expressions for dimensionless parameters. Values correspond to the SL with $\Delta = 97.99$ meV in table 3.

Variable	Scale	Value
x	$\varepsilon F_M l / (e N_D)$	14 nm
k	$1/l$	0.21 nm ⁻¹
t	$\varepsilon F_M l / (e N_D v_M)$	0.19 ps
F	F_M	20 kV cm ⁻¹
n, f	N_D	10 ¹⁷ cm ⁻³
μ	$k_B T$	300 K
J, J_0	$e N_D v_M / l$	1.28 × 10 ⁵ A cm ⁻²
ν	v_M	80 km s ⁻¹

Parameter	Expression	Value
ϵ	$\hbar v_M N_D / (\varepsilon F_M^2 l^2)$	0.38
δ	$\Delta / (2 k_B T)$	1.89
$\tau_{e,i}$	$e F_M l / (\hbar \nu_{e,i})$	$\sqrt{2}$

Table 3. Structural data and calculated miniband width Δ for SLs in [13].

Δ (meV)	Well (Å)	Barrier (Å)	Length (μm)	Doping (10 ¹⁷ cm ⁻³)
54.75	51.3	8.7	0.60	1.4
58.61	48	9	0.57	0.8
73.06	40	10	0.5	0.8
97.99	36.4	9.3	0.64	1
98.31	35.4	9.6	0.45	0.9

To approximate the kinetic equation, we use the Chapman–Enskog method [15]. In this technique, we expand the distribution function and the rate equation for the electron density in powers of a book-keeping parameter ϵ that will be set equal to 1 at the end of the process:

$$f(x, k, t; \epsilon) = f^{(0)}(k; n) + \sum_{m=1}^{\infty} f^{(m)}(k; n) \epsilon^m, \quad (7)$$

$$\frac{\partial n}{\partial t} = \sum_{m=0}^{\infty} N^{(m)}(n) \epsilon^m. \quad (8)$$

The coefficients $f^{(m)}(k; n)$ depend on the ‘slow variables’ x and t only through their dependence on the electron density and the electric field (which is itself a functional of n). The electron density obeys a reduced evolution equation (8) in which the functionals $N^{(m)}(n)$ are chosen so that the $f^{(m)}(k; n)$ are bounded and $2\pi/l$ -periodic in k . An explicit expression can be easily obtained. We integrate equation (1) with respect to k , thereby getting the charge continuity equation

$$\frac{\partial n}{\partial t} = -\frac{l}{2\pi} \frac{\partial}{\partial x} \int_{-\pi/l}^{\pi/l} v(k) f^{(m)}(x, k, t) dk. \quad (9)$$

Inserting (7) into this equation, we obtain

$$\begin{aligned} N^{(m)} &= -\frac{l}{2\pi} \frac{\partial}{\partial x} \int_{-\pi/l}^{\pi/l} v(k) f^{(m)}(x, k, t) dk \\ &= \frac{\Delta l}{2\pi} \frac{\partial}{\partial x} \text{Im} f_1^{(m)}(x, t). \end{aligned} \quad (10)$$

Equations (2), (8) and (10) yield the following evolution equation for the electric field:

$$\varepsilon \frac{\partial F}{\partial t} = \frac{e \Delta}{2\hbar} \sum_{m=0}^{\infty} \epsilon^m \text{Im} f_1^{(m)} + J(t), \quad (11)$$

in which the ‘integration constant’ $J(t)$ is the total current density through the SL.

To find the functions $f^{(m)}$, we insert (7) and (8) in the Boltzmann equation (1) and equate like powers of ϵ . The result is a hierarchy of linear equations for the $f^{(m)}$, $m = 0, 1, \dots$. For $m \geq 1$, these linear equations are inhomogeneous and they have bounded and periodic solutions (in k), provided certain solvability conditions hold. These conditions also yield (10). Solving the linear equations of the hierarchy, we obtain the unknown functions $f_1^{(m)}$, $m = 0, 1, \dots$ to be inserted in equation (11). If we keep in equation (11) terms up to order ϵ^2 , and then set $\epsilon = 1$, the result is the following *generalized drift-diffusion equation* (GDDE) [11]:

$$\begin{aligned} \epsilon \frac{\partial F}{\partial t} + \mathcal{V} \left(F, \frac{\partial F}{\partial x} \right) \frac{eN_D}{l} \left(1 + \frac{\epsilon l}{eN_D} \frac{\partial F}{\partial x} \right) \\ = D \left(F, \frac{\partial F}{\partial x} \right) \epsilon \frac{\partial^2 F}{\partial x^2} + A \left(F, \frac{\partial F}{\partial x} \right) J(t), \end{aligned} \quad (12)$$

where we have introduced the following variable coefficients:

$$A = 1 + \frac{2ev_M F_M^3 [F_M^2 - (1 + 2\tau_c^2) F^2]}{\epsilon l (v_e + v_i) (F_M^2 + F^2)^3} n \mathcal{M}, \quad (13)$$

$$\mathcal{V} = v_M V \mathcal{M} \left\{ A - \frac{\Delta B}{2e} \frac{\partial F}{\partial x} \right\}, \quad (14)$$

$$D = \frac{\Delta^2 l F_M}{8\hbar e \tau_c (F_M^2 + F^2)} \left(1 - \frac{4\hbar v_M C}{\Delta l} \right), \quad (15)$$

$$\begin{aligned} B = \frac{(5F_M^2 - 4F^2) \mathcal{M}_2}{(F_M^2 + 4F^2)^2 \mathcal{M}} \\ - \frac{4\hbar v_M F_M^2 (F_M^2 - F^2) (\tau_c + \tau_c^{-1})}{\Delta l (F_M^2 + F^2)^3} \frac{\partial(n\mathcal{M})}{\partial n}, \end{aligned} \quad (16)$$

$$C = \frac{\tau_c (F_M^2 - 2F^2)}{F_M^2 + 4F^2} \frac{\partial(n\mathcal{M})}{\partial n} + \frac{8\hbar v_M (F F_M)^2}{\Delta l (F_M^2 + F^2)^2} \left[\frac{\partial(n\mathcal{M})}{\partial n} \right]^2, \quad (17)$$

and the following functions and values:

$$V(F) = \frac{2F}{1 + F^2}, \quad v_M = \frac{\Delta l}{4\hbar \tau_c} \frac{\mathcal{I}_1(M)}{\mathcal{I}_0(M)},$$

$$F_M = \frac{\hbar \sqrt{v_e(v_e + v_i)}}{el}, \quad \tau_c = \sqrt{\frac{v_e + v_i}{v_e}},$$

$$\mathcal{M}(n) = \frac{\mathcal{I}_1(\mu/k_B T) \mathcal{I}_0(M)}{\mathcal{I}_1(M) \mathcal{I}_0(\mu/k_B T)},$$

$$\mathcal{M}_2(n) = \frac{\mathcal{I}_2(\mu/k_B T) \mathcal{I}_0(M)}{\mathcal{I}_1(M) \mathcal{I}_0(\mu/k_B T)},$$

$$\mathcal{I}_m(s) = \int_{-\pi}^{\pi} \cos(mk) \ln(1 + e^{s - \delta + \delta \cos k}) dk,$$

$$\delta = \frac{\Delta}{2k_B T}.$$

Equation (12) is strongly nonlinear because $\mathcal{M}(n)$ and $\mathcal{M}_2(n)$ depend nonlinearly on $\partial F/\partial x$ through their definitions, the Poisson equation (2) and the electrochemical potential $\mu(n)$. Except for a different notation, $D(F, O)$ in equation (15) coincides with the diffusion coefficient found by Ignatov and Shashkin in their linear stability analysis of the uniform field profile for equation (1) in the high temperature limit and with $v_i = 0$, [24].

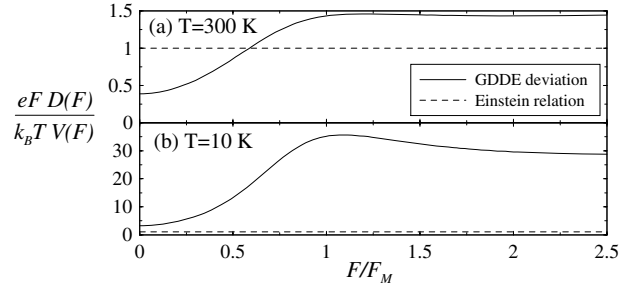


Figure 1. Deviation of GDDE from the Einstein relation for $N_D = 3 \times 10^{17} \text{ cm}^{-3}$ and $l = 4.9 \text{ nm}$. (a) Room temperature (300 K), and (b) low temperature (10 K).

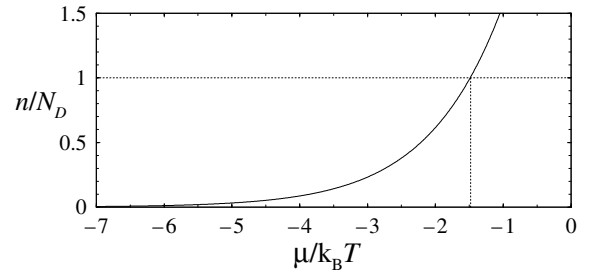


Figure 2. Electron density versus chemical potential for the superlattice with $\Delta = 97.99 \text{ meV}$ in table 3. Dotted lines indicate $\mu/k_B T (n = N_D) \equiv M = -1.48$.

Notice that our GDDE has been consistently derived from the kinetic equation, which is rather different from the usual *ad hoc* arguments, that employ the Esaki–Tsu velocity and the diffusion coefficient obeying the Einstein relation. Moreover, the *drift velocity and the diffusion coefficient in the GDDE* (12) do not satisfy the Einstein relation [11]. Figure 1 shows that such deviation is important for the two typical values of the temperature: at room temperature ($T = 300 \text{ K}$) the deviation is of the order of the magnitude itself, and one order greater at low temperature ($T = 10 \text{ K}$).

3. Solutions: travelling field domains and current density oscillations

One of the main technological interests of superlattices is to obtain high-frequency current oscillations that can be tuned by changing the applied bias. To study this possibility, we compare the numerical solution of the model with the experimental results by Schomburg *et al* [13] on different GaAs/AlAs SLs.

3.1. Values of the parameters

To solve the system (12)–(17) it is necessary to find the relation between the electrochemical potential μ and the electron density n . This relation is then used to evaluate the integrals $\mathcal{I}_m(\mu/k_B T)$. We obtain $\mu(n)$ by solving graphically equation (3), as is indicated in figure 2. For $n = N_D$ we find $\mu/k_B T \equiv M$.

The miniband width Δ has been calculated using the Kronig–Penney model, which assumes that there is a unique effective electron mass and that wavefunctions $\Psi(x)$ and their derivatives are continuous. Another possibility is to assume

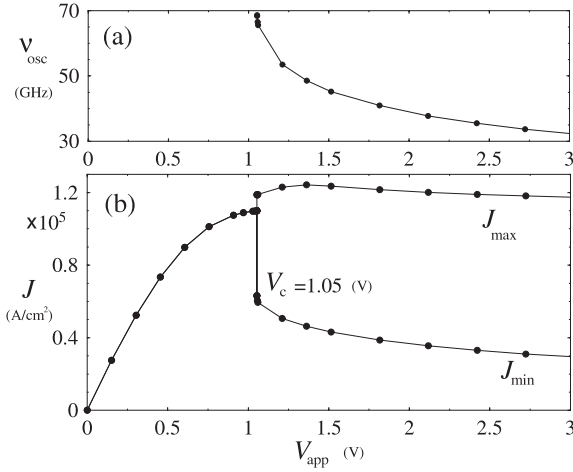


Figure 3. I - V characteristic $J(V_{\text{app}})$ for SL with $\Delta = 97.99$ meV in table 3. (a) Frequency of oscillation versus applied voltage, with the onset of oscillations located at $V_c \approx 1.05$ V. (b) Maximum (upper branch) and minimum (lower branch) of current density versus applied voltage.

different effective masses of GaAs and AlAs and continuity of $m^{*-1}\partial\Psi(x)/\partial x$ [17]. This latter calculation yields worse results for the miniband width, as shown by Sibille [18], so that we use the Kronig–Penney model. Results for the simulated superlattices are shown in table 3.

We assume $\nu_{e,i} = 0.1$ ps, which agrees with earlier theoretical results [19, 20]. This is also the value of the estimated optical phonon scattering time referred to in [21], from which we also take the values of the effective mass and dielectric constant of GaAs: $m^* = 0.063m_0$ and $\varepsilon = 13.2\varepsilon_0$. Here m_0 and ε_0 are the electron rest mass and the vacuum permittivity, respectively. For the sake of simplicity, the temperature dependence is ignored.

We then solve our model for the SLs used in the experiments of Schomburg *et al*; see again table 3.

3.2. Numerical simulations

Despite its formidable appearance, the GDDE (12) is (in dimensionless units) a small perturbation of the drift equation $\partial n/\partial t = N^{(0)}$, analysed in studies of the Gunn effect [16]. We have solved it numerically by means of an efficient scheme in finite differences often used in integro-differential problems similar to models of the Gunn effect [22].

We solve the GDDE (12) together with the bias condition $\int_0^L F(x, t) dx = V_{\text{app}}$ for the electric field profile $F(x, t)$ and the current density $J(t)$. Here L is the length of the SL and V_{app} is the applied voltage. Boundary conditions are $F(0, t) = F(L, t) = J(t)/\sigma$ (ohmic contacts), in which σ is the conductivity of the contacts. For simplicity, we take the same value at both contacts ($\sigma = 0.5$ in dimensionless units). Initial conditions $F(x, 0)$ and $J(0)$ are such that bias and boundary conditions are verified.

Our model reproduces the values of the oscillation frequency of each specific SL in Schomburg *et al*'s experiments [13]. Figure 3 shows the oscillation frequency ν_{osc} as a function of the applied voltage V_{app} and the $J(V_{\text{app}})$ characteristic curve for the SL with $\Delta = 97.99$ meV in table 3.

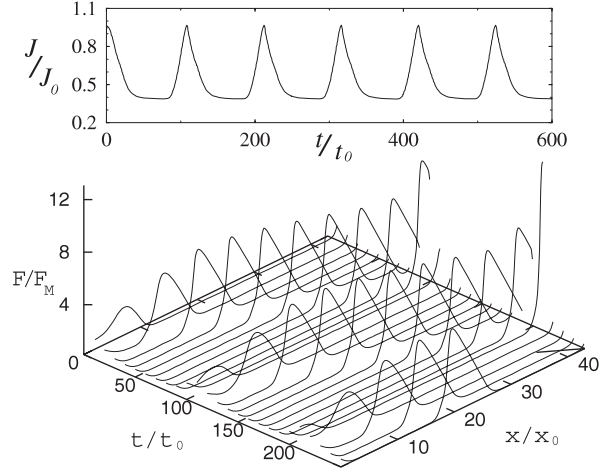


Figure 4. Current oscillations (upper) and travelling dipole domain propagating from cathode to anode (lower) in the SL $\Delta = 97.99$ meV with $L = 0.64 \mu\text{m}$ at $V_{\text{app}} \approx 1.24$ V.

Table 4. Numerical values of the oscillation frequencies $\nu_{\text{osc}}^{\text{NUM}}$, compared with the experimental value $\nu_{\text{osc}}^{\text{EXP}}$ for five of the SLs of [13], together with the corresponding applied voltage V_{app} .

Δ (meV)	$\nu_{\text{osc}}^{\text{EXP}}$ (GHz)	$\nu_{\text{osc}}^{\text{NUM}}$ (GHz)	V_{app} (V)
54.75	19.44	19.5	0.95
58.61	29.12	29.1	1.07
73.06	46.35	46.5	1.2
97.99	52.79	52.8	1.24
98.31	≈ 65	65	1.73

The SL exhibits a stationary regime for values of V_{app} under a critical voltage V_c at which the oscillatory regime begins. Above V_c , the current density oscillates between an almost constant maximum value $J_{\text{max}}(V_{\text{app}})$ and a slightly decreasing minimum value $J_{\text{min}}(V_{\text{app}})$. At $V_{\text{app}} \approx 1.24$ V the oscillation frequency $\nu_{\text{osc}}^{\text{NUM}}$ is about 52 GHz, very similar to the experimental value: $\nu_{\text{osc}}^{\text{EXP}} = 52.79$ GHz. Good agreement with experiments also occurs for the other SLs in [13], as indicated in table 4.

Figure 4 depicts the current oscillations and the corresponding electric field profile evolution. The behaviour of the SL is very similar to the one observed in the Gunn effect. During each period of the oscillations, a field domain is nucleated near the cathode and advances in the interior of the SL with constant shape and velocity, until it reaches the anode and disappears there, producing a peak in the current density curve. Then a new wave is nucleated and a new period of the oscillation starts.

For large samples, such as those in experiments, the current oscillations correspond to a periodic motion of a dipole wave which dies before reaching the anode, as is shown in figure 5. This situation is well understood in bifurcation studies of the Gunn effect [23]. If the SL length is smaller than a critical value, the dipoles always reach the anode.

4. Summary

In this paper we have presented an asymptotically consistent derivation of a drift-diffusion model for strongly coupled

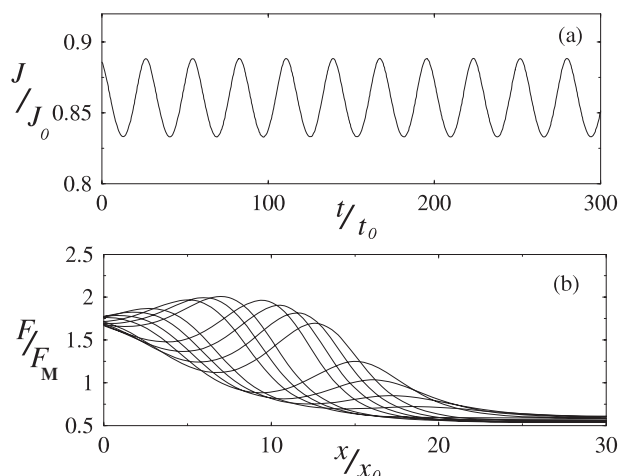


Figure 5. Numerical simulation for the SL with $\Delta = 54.75$ meV at $V_{\text{app}} = 0.72$ V just above V_c . (a) Small-amplitude current density sinusoidal oscillations and (b) electric field wave disappearing near the cathode region, as described in [23] for the Gunn effect. Note that not all the sample is depicted here.

SLs starting from a semiclassical Boltzmann–Poisson system. The main facts to stress are the consistency of the derivation and that the Einstein relation between drift velocity and diffusivity does not hold. We have solved the model numerically and found results that agree with experimentally observed ones [13], particularly with frequencies. Simulations show that these frequencies increase with miniband width and can be tuned by changing the bias until values over 70 GHz are reached.

Acknowledgments

This work has been supported by the MCyT grant BFM2002-04127-C02-01, and by the European Union under grant HPRN-CT-2002-00282.

References

- [1] Esaki L and Tsu R 1970 *IBM J. Res. Dev.* **4** 61
- [2] Grahn H T (ed) 1995 *Semiconductor Superlattices: Growth and Electronic Properties* (Singapore: World Scientific)
- [3] Bonilla L L 2002 *J. Phys.: Condens. Matter* **14** R341
- [4] Wacker A 2002 *Phys. Rep.* **357** 1
- [5] Sibille A, Palmier J F, Wang H and Mollot F 1990 *Appl. Phys. Lett.* **56** 256
- [6] Büttiker M and Thomas H 1977 *Phys. Rev. Lett.* **38** 78
- [7] Lei X L, Horing N J M and Cui H L 1991 *Phys. Rev. Lett.* **66** 3277
- [8] Lei X L 1995 *Phys. Rev. B* **51** 5184
- [9] Scheuerer R, Schomburg E, Renk K F, Wacker A and Schöll E 2002 *Appl. Phys. Lett.* **81** 1515
- [10] Kroemer H 1966 *IEEE Trans. Electron Devices* **13** 27
- [11] Bryksin V V and Kleinert P 2003 *J. Phys.: Condens. Matter* **15** 1415
- [12] Bonilla L L, Escobedo R and Perales A 2003 *Phys. Rev. B* **68** 241304(R)
- [13] Bhatnagar P L, Gross E P and Krook M 1954 *Phys. Rev.* **94** 511
- [14] Schomburg E, Blomeier T, Hofbeck K, Grenzer J, Brandl S, Lingott I, Ignatov A A, Renk K F, Pavelev D G, Koschurinov Y, Melzer B Y, Ustinov V M, Ivanov S V, Zhukov A and Kopev P S 1998 *Phys. Rev. B* **58** 4035
- [15] Higuera F J and Bonilla L L 1992 *Physica D* **57** 161
- [16] Bonilla L L 2000 *Phys. Rev. E* **62** 4862
- [17] Knight B W and Peterson G A 1966 *Phys. Rev.* **147** 617
- [18] Bastard G 1988 *Wave Mechanics Applied to Semiconductor Heterostructures* Les Éditions de Physique (New York: Halsted Press)
- [19] Sibille A 1995 Miniband transport *Semiconductor Superlattices: Growth and Electronic Properties* ed H T Grahn (Singapore: World Scientific) pp 31–2
- [20] Capasso F, Mohammed K and Cho A Y 1986 *Appl. Phys. Lett.* **48** 478
- [21] Ferreira R and Bastard G 1989 *Phys. Rev. B* **40** 1074
- [22] Grahn H T 1999 *Semiconductor Physics* (Singapore: World Scientific)
- [23] Carpio A, Hernando P J and Kindelan M 2001 *SIAM J. Numer. Anal.* **39** 168
- [24] Bonilla L L and Higuera F J 1995 *SIAM J. Appl. Math.* **55** 1625
- [25] Ignatov A A and Shashkin L 1984 *Fiz. Tekh. Poluprovodn.* **18** 721 (*Sov. Phys. Semicond.* **18** 449)